Plug-and-play microvalve and micropump for rapid integration with microfluidic chips

Citation: Shaegh, Seyed Ali Mousavi, Zhenfeng Wang, Sum Huan Ng, Ruige Wu, Huu Tuan Nguyen, Leon Cong Zhi Chan, Alicia Guek Geok Toh, and Zhiping Wang. "Plug-and-Play Microvalve and Micropump for Rapid Integration with Microfluidic Chips." Microfluid Nanofluid 19, no. 3 (April 22, 2015): 557–564.

As Published: http://dx.doi.org/10.1007/s10404-015-1582-4

Publisher: Springer Berlin Heidelberg

Persistent URL: http://hdl.handle.net/1721.1/103131

Version: Author's final manuscript: final author's manuscript post peer review, without publisher's formatting or copy editing

Plug-and-play microvalve and micropump for rapid integration with microfluidic chips

Seyed Ali Mousavi Shaegh,*[a§] Zhenfeng Wang,*[a] Sum Huan Ng,[a] Ruige Wu,[a] Huu Tuan Nguyen,[b] Leon Cong Zhi Chan,[a] Alicia Guek Geok Toh,[a] Zhiping Wang,[a]

[a]Singapore Institute of Manufacturing Technology

[b]Nanyang Technological University, Singapore

*Corresponding email: mousavi@mit.edu , a.m.shaegh@gmail.com (Seyed Ali Mousavi Shaegh); zfwang@simtech.a-star.edu.sg (Zhenfeng Wang)

§Current address: Harvard-MIT Division of Health Sciences and Technology, Massachusetts Institute of Technology, Cambridge, MA 02139, USA

Abstract

This paper reports design, fabrication and characterization of an air-actuated microvalve and a micropump made of thermoplastic materials. The bonding process was carried out by thermal fusion process with no particular surface treatment. The developed microvalve was used as a reversible switch for controlling both liquid flow and electrical field. Bonding strength of the fabricated microvalves could withstand of liquid and air pressures of up to 600 kPa with no burst failure. The micropump made of three connected microvalves, actuated by compressed air, could generate a liquid flow rate of up to 85 µl/min. The proposed microvalve and micropump can be used as pre-fabricated off-the-shelf microfluidic functional elements for easy and rapid integration with thermoplastic microfluidic circuitries in a plug-and-play arrangement.

Introduction

Because of essential role of flow control and manipulation for microfluidic applications, many investigations have been carried out to develop various designs of microvalves (Oh and Ahn 2006; Zhu et al. 2012; Jiang and Erickson 2013; Kang et al. 2013; Shiraki et al. 2015) and micropumps (Nguyen et al. 2002; Yobas et al. 2008; Qin et al. 2009; Zhang et al. 2015). Examples of deploying microvalves can be found for cell culture assays (Gómez-Sjöberg et al. 2007; Wu et al. 2008; Frimat et al. 2011), microfluidic drug screening (Ma et al. 2009; Nguyen et al. 2013), single cell analysis (Irimia 2010) and droplet microfluidics (Zeng et al. 2009). Silicon-based microvalves and micropumps were developed at the early stages of microfluidic progress using surface and bulk micromachining technologies (Oh and Ahn 2006). But for the last 15 years, different polymers have been adopted for development of microvalves and micropumps taking advantage of cheaper materials and easier fabrication methods.

Generally, a microvalve is made of a flexible diaphragm sandwiched between a control chamber and a liquid chamber (control chamber/diaphragm/liquid chamber). Upon the deformation of the diaphragm by an external means, flow inside the fluidic chamber can be manipulated. In terms of fabrication process, microvalves are generally categorized into (i) built-in microvalves and (ii) pre-fabricated microvalves. For built-in microvalves, diaphragm is generally made of PDMS. Control chambers and the liquid chambers can be made of Polydimethylsiloxane (PDMS), Polymethylmethacrylate (PMMA) and Cyclic Olefin Copolymer (COC) during the course of chip fabrication in the following arrangements: (PDMS/PDMS/PDMS) (Unger et al. 2000; Gómez-Sjöberg et al. 2007; Gu et al. 2010), (PMMA/PDMS/PMMA)(Zhang et al. 2009), and (COC/PDMS/COC) (Gu et al. 2010). Because of small footprint of such microvalves, e.g. 100 µm×100 µm (Unger et al. 2000), built-in microvalve concept enables Microfluidic Large-scale Integration (Melin and Quake 2007) with pneumatic actuation, suitable for high throughput cell culture and single cell analysis (Wu et al. 2004; Gómez-Sjöberg et al. 2007; Lii et al. 2008).

It has been reported that PDMS with no surface treatment can absorb some small hydrophobic molecules, i.e. estrogen, during microfluidic drug screening (Regehr et al. 2009; Berthier et al. 2012). In addition, some uncured oligomer compounds from the polymeric network of PDMS can leach into the microchannel media affecting cell membrane during cell culture (Regehr et al. 2009; Berthier et al. 2012). Also, some organic solvents swell PDMS or dissolve PDMS compounds (Lee et al. 2003). Such features of PDMS can hinder some applications, particularly microfluidic organ-on-chip devices for drug screening. In order to mitigate the mentioned problems of using PDMS for microvalve fabrication, other elastomers including Teflon (Teflon/Teflon/Teflon) (Grover et al. 2008), Viton®

(PMMA/Viton®/PMMA) or (COC/Viton®/COC) (Ogilvie et al. 2011) have been explored for built-in microvalves.

Pre-fabricated microvalves (Elizabeth Hulme et al. 2009) can be made in advance and then integrated with a pre-fabricated microfluidic chip. In contrast to built-in microvalves, these microvalves have larger footprints at millimetre scale. Therefore, because of ease of incorporation, such microvalves are suitable for plug-and-play applications where low-density integration of microfluidic components is required. Some explored applications are gradient generators (Elizabeth Hulme et al. 2009), immunoassay (Weibel et al. 2005) and on-chip lifelong observation of *C. elegans* (Hulme et al. 2010).

Depending on the microvalve design, a pre-fabricated microvalve can be actuated manually by a screw (Weibel et al. 2005; Hulme et al. 2010), electrically by a solenoid actuator (Weibel et al. 2005), or pneumatically (Elizabeth Hulme et al. 2009). Pre-fabricated valves are mainly made of PDMS in large quantities. They are embedded into microfluidic chips during the casting of the master made of PDMS (Hulme et al. 2010). Pre-fabricated valves made from PDMS are suitable for PDMS-based microfluidic devices. Therefore, there is a lack of microvalves for user-friendly integration with microfluidic chips made of thermoplastic materials.

In recent years, thermoplastic materials have gained significant popularity for microfluidic applications (Tsao and DeVoe 2009) suitable for high volume, low-cost production (Chin et al. 2012). Also, they have lower oxygen permeability compared to PDMS (Ochs et al. 2014). Materials with low oxygen permeability are required for making devices to create oxygen-controlled conditions on a microfluidic chip for tumour microenvironment and hypoxia (Byrne et al. 2014).

In this paper, we reported a systematic approach for design, fabrication and characterization of a plug-and-play pre-fabricated microvalve and a micropump for easy integration with microfluidic chips made of thermoplastic materials. As shown in Figure 1, the normally-open microvalve was made of a flexible diaphragm, thermoplastic polyurethane (TPU), sandwiched between a liquid chamber and an air chamber both made of PMMA. Upon increasing air pressure inside the control chamber, the diaphragm was deformed downwards at the liquid chamber (displacement chamber) to stop the liquid passing through the microvalve. Different layers of microvalve were bonded together through thermal fusion process with no particular surface treatment.

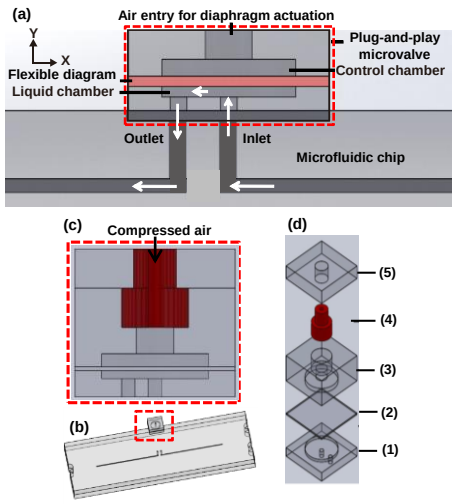

Figure 1. (a) Concept design of the plug-and-play microvalve for integration with thermoplastic microfluidic chips, (b) schematic of the microvalve-chip assembly, (c) a cross-sectional view of the microvalve with an embedded connector, (d) an exploded view of the microvalve: (1) bottom component to accommodate liquid chamber, (2) TPU flexile diaphragm, (3) intermediate component to accommodate the air chamber and the embedded connector, (4) the embedded connector and (5) top component

Valve design

Single microvalve module was designed based on using five components, Figure 1(b)-1(d). Components No. (1), (3), and (5) were fabricated using micromilling process out of PMMA. Both liquid and air chambers are designed to have a diameter of 4 mm. Upon applying pressure, the

diaphragm sandwiched between the bottom and the intermediate components was deformed downwards at the liquid chamber (displacement chamber) to block the inlet port, which was located at the center of the fluidic chamber. Spacing between the inlet port and the outlet port was set to be 1.0 mm. Such design enables the microvalve to be integrated with a microfluidic chip easily using different bonding techniques including thermal bonding, ultrasonic welding or adhesive bonding. The microvalve can be implemented on a microfluidic chip in a plug-and-play manner by linking its inlet and outlet ports to the corresponding ports of a fluidic channel embedded in the microfluidic chip, Figure 1. For an easy chip-to-world connection, a connector made of silicone rubber was made and embedded within the microvalve structure. The connector was used to connect the microvalve a compressed air regulator for valve actuation.

Material selection

Micromilling process was used to make the circular control and liquid chambers from Poly(methyl methacrylate), PMMA. PMMA has been widely used for rapid prototyping of microfluidic chips by micromilling method and laser ablation techniques (Waldbaur et al. 2011). Also, it can be injection molded (Becker and Gärtner 2008) for the mass production of commercialized chips. An off-the-shelf thermoplastic polyurethane (TPU) film with a thickness of 150±15 µm, Bothane 85A (Texin®) from BAYER®, was selected for making the flexible diaphragm. Polyurethane elastomers have gained significant attentions for microfluidic chip fabrication (Piccin et al. 2007; Wu et al. 2012; Gu et al. 2013). They have high-mechanical strength, resiliency, and good resistance to abrasion. (Gu et al. 2013). Also, glass transition temperature (T_g) of TPU film was measured. Dynamic Mechanical Thermal analysis upon heating from -120 ºC to 140 ºC revealed that TPU has a low T_g of -50 ºC while T_g of PMMA is generally reported around 110 ºC. In addition, TPU film was optically characterized. High light absorbance at infrared wavelengths of 6 µm to 11 µm in transmittance measurement was observed. This optical property of TPU film makes it a suitable material for ablation and cutting using CO_2 laser beam which has an inherent wavelength of 10.6 µm (Hong et al. 2010).

Numerical simulation and experimental validation of diaphragm deflection

Finite Element Method (FEM) using ANSYS 11.0 software was used to simulate the deflection of the circular diaphragm under different air pressures. All geometries, forces and boundary conditions were axisymmetric, therefore a two-dimensional (2-D) and 8-node element axisymmetric model was established in ANSYS to mesh the computational domain.

In order to establish the FEM model, we run a uniaxial tension test on our TPU film to understand its strain-stress characteristics. TPU film showed a nonlinear hyperelastic property, and Mooney-Rivlin (9 parameters) constitutive model was exploited to fit the data. Diameter of liquid and control chambers was set at 4 mm. The following boundary conditions and assumptions were considered to simulate the diaphragm deformation at the computational domain:

- Axisymmetric setup with respect to the centre of the valve geometry
- Displacement in the horizontal direction constrained along the axis of symmetry
- All degrees of freedom constrained on the bottom surface of the microvalve seat
- Load was applied as a uniformly-distributed pressure on the top surface of the membrane
- Contact elements condition used to simulate the contact conditions at the diaphragm-valve seat interface

For contact elements condition, a friction coefficient of 0.1 was considered for diaphragm-valve seat interface. Large displacement static option was used to solve the model.

In order to evaluate the predications for diaphragm deformation obtained from FEM model, a test chip was fabricated where the diameter of the test chip diaphragm was the same as diaphragm diameter of the FEM model (4 mm), Figure 2(a) and 2(b). The test chip was made of a TPU film sandwiched between two PMMA slabs through thermal boding process. As shown in Figure 2(c), the test chip enabled the measurement of diaphragm deflection under different air pressures for comparison with the results obtained from the FEM analysis. Three diaphragms were tested. In the experiment, the vertical deflection was measured optically at the central point of the diaphragm using a ZETA-20 3D Imaging & Metrology System. In general, the FEM predictions have similar trends with the experimental results. Both FEM and experimental results show that the diaphragm deflection increases with pressure. Experimental results showed higher deflections than the FEM model predictions and they are characterised by offsets in the vertical direction. Upon examination of the diaphragms, it was noticed

that there were initial warpage of the diaphragm introduced by the process of bonding the TPU diaphragm to PMMA test chip. This initial warpage may lead to a higher deflection compared to a flat membrane. Figure 2(c) shows a displacement result obtained from FEM model when the diaphragm was subjected to a pressure of 35 kPa. The periphery of the diaphragm was constrained from displacing downwards. But the central region showed the largest displacement of ~300 µm causing it to just come into contact with the edge of the inlet hole. The inlet was located at the centre of the microvalve seat inside the liquid chamber.

Figure 3 shows FEM prediction of contact pressure between the diaphragm and the valve seat at pressures of 40 kPa and 100 kPa. At 40 kPa, a contact region around the periphery of the inlet hole was formed as the diaphragm pressed against it. The width of the contact ring was about 50 µm with a peak in the contact pressure distribution at the edge of the hole. When the pressure was increased to 100 kPa, the width of the contact ring increased to about 450 µm. The peak due to the sharp edge of the hole was still there. Most of the contact region maintained a contact pressure of over 100 kPa which was essential for leakage-free sealing.

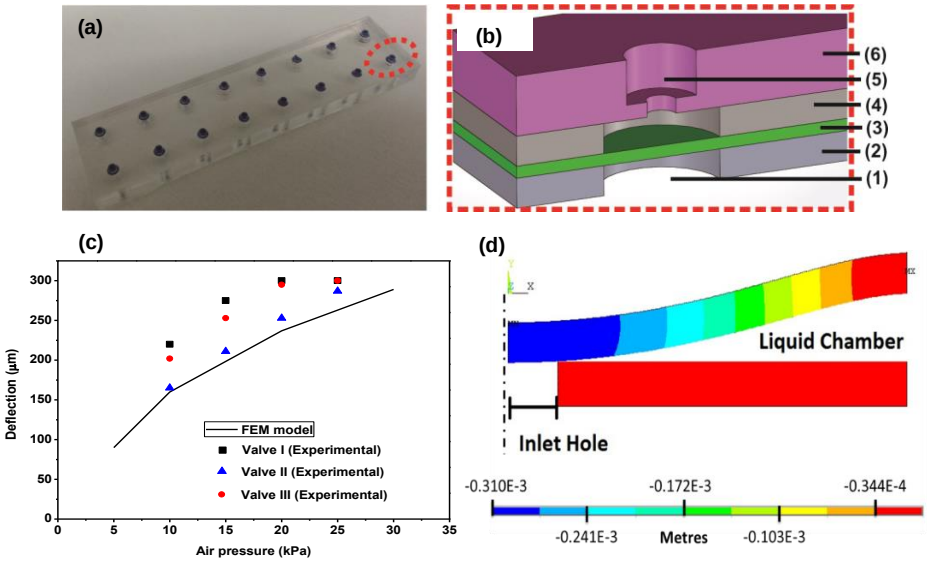

Figure 2. (a) Fabricated test chip for measuring diaphragm deflection under different air pressures, (b) detailed schematic of the test chip: (1) window for microscopy (2) PMMA layer (3) TPU diaphragm (4) PMMA layer (5) air entry for diaphragm actuation and (6) PMMA layer for embedded connector, (c) experimental characterization results for three diaphragms of the test chip shown in (a) in comparison with FEM analysis of membrane deflection versus different applied air pressures, (d) 2-D axisymmetric FEM analysis showing deflection of the microvalve diaphragm under a pressure of 35 kPa applied uniformly to the top of the diaphragm. The bottom of the membrane was seen to be just touching the edge of the inlet hole. Legend unit: meters.

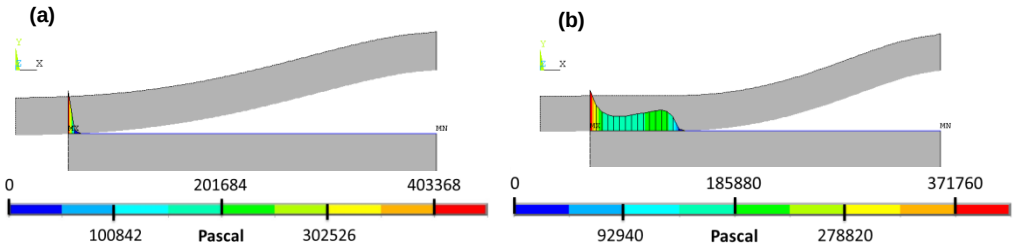

Figure 3. Contact pressure between the flexible diaphragm and the valve seat from FEM simulation; (a) at 40 kPa pressure, (b) at 100 kPa pressure. Legend units: Pascal.

Valve fabrication

Since both PMMA and TPU were thermoplastic, the fabrication of the whole valve module took advantage of direct thermal bonding technique with no intermediate adhesive. PMMA components were fabricated using micromilling process while TPU films were cut either using CO_2 laser beam or a blade cutter at circular shapes.

The thermal bonding process was comprised of two major steps: thermal pre-treatment step and low pressure bonding step where components were bonded together using a metallic jig. During the thermal pre-treatment process, surface of PMMA components and TPU films were cleaned by Isopropyl Alcohol (IPA) and then blown by filtered air. They were subsequently kept in a vacuum oven at 80 ºC for 24 hours to facilitate the removal of any volatile residuals from the components. After 24 hours, TPU film was removed from the vacuum oven and its surface was cleaned thoroughly again using cleanroom wiper and IPA and DI water followed by air blow to remove any residuals and debris. Then it was returned back to the vacuum oven and kept for at least 6 hours. This thermal pre-treatment can enhance the strength and quality of the bonding at the low pressure bonding step. The thermally-treated PMMA components and the TPU film were removed from the oven and then aligned on top of each other accordingly. The assembled components were sandwiched in a metallic jig for thermal bonding process. Subsequently, the whole assembly was put in the oven (Memmert, model UFE600). It was heated and then kept at temperature of 115 ºC for 60 minutes. Then the assembly was cooled down to 60 ºC within 60 minutes. The metallic jig had adjustable screws to control the bonding pressure. The applied torque to adjust the screw was 1 N.m. Inspection after bonding process was carried out for any visible distortion, crack or delamination of multiple layers of the fabricated valves.

Valve characterization

As shown in Figure 4, fabricated valves were tested on a test chip to visualize the diagram deformation upon applying pressurized air to the control chamber. Also, a pressure test set-up was designed and fabricated to examine microvalve operation and mechanical strength of thermal bonding of TPU to PMMA under different operating pressures. It was observed that the bonding strength of PMMA/TPU/PMMA was sufficient to withstand liquid and air pressures of up to 500 kPa with no burst failure. As shown in Figure 5, characterization experiments were carried out for control air pressures of 100 kPa, 200 kPa and 300 kPa. Leakage-free operations at liquid pressures lower than the air pressure was realized. It was observed that when the pressure of liquid approached to the pressure of actuating air, liquid started to leak through the diaphragm-valve seat interface.

The function of the microvalve was also demonstrated in an electrical isolation test as a reversible electrical switch. As shown in Figure 6, a microvalve was integrated onto an electrophoresis chip. To start with the characterization test, channel was filled up with TAE buffer solution (40 mM Tris, 20 mM acetic acid, 1 mM EDTA, pH 8.3). Then the whole channel between the inlet and the outlet was filled with a 0.5% agarose gel. After gel solidified, a 1 kb DNA ladder, from 250 to 10000 base pairs, mixed SYBR green I (100X) was deposited on top of the inlet. A potential of 110 V was applied to electrodes and DNA band travelled 6.5 mm toward the positive electrode in 18 minutes. Then the microvalve kept closed for 6 minutes by applying an air pressure of 250 kPa. During this period, it was observed that the leading edge of the DNA band showed a minor move of less than 0.1 mm, which can be attributed to diffusion phenomenon. After that, pressurized air was cut off made to make the valve open and a movement of 2.4 mm was observed within 6 minutes. This observation indicated that the air-actuated microvalve was able to isolate two adjacent fluidic chambers as a reversible electrical switch.

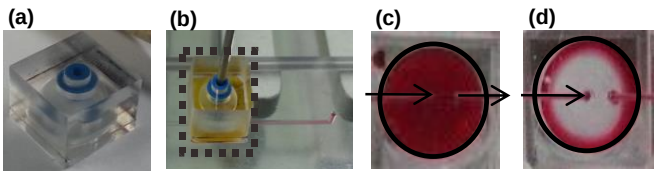

Figure 4. (a) An individual fabricated microvalve, (b) integrated microvalve on the test chip using a double adhesive Kapton tape, (c) liquid chamber of the valve shown in (b) before diaphragm actuation, (d) liquid chamber of the valve shown in (b) after actuation under 100 kPa air pressure.

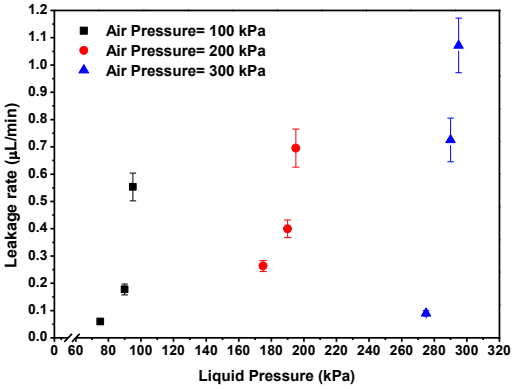

Figure 5. Microvalve leakage rate vs. liquid pressure under different actuation air pressures.

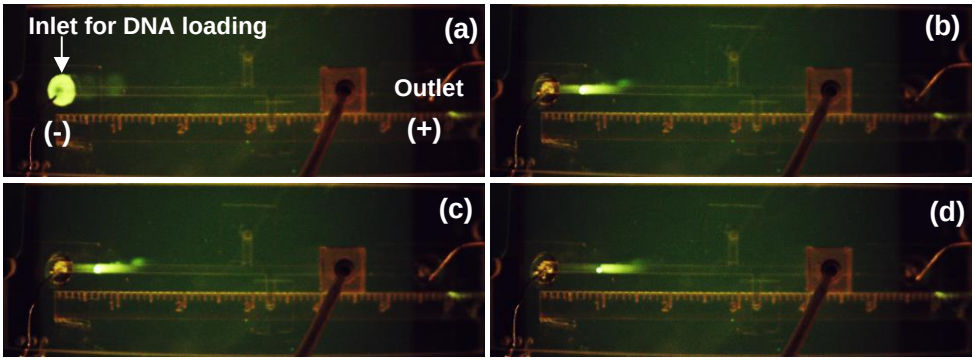

Figure 6. DNA electrophoresis chip with integrated valve. For all figures voltage is 110 V AC. (a) Start time (t = 0), microvalve open, (b) after 18 minutes, valve open, DNA band travelled 6.5 mm, (c) after 24 minutes, microvalve kept closed for 6 minutes, (e) after 30 minutes, valve was open for 6 minutes, DNA travelled 2.4 mm.

Plug-and-play peristaltic micropump

Making use of the microvalve design, a peristaltic pumping scheme was achieved by consecutive integration and operation of three interconnected liquid chambers integrated on a substrate. The working principle of the micropump was based on the deflection of three TPU diaphragms actuated by three air entries on top of the diaphragms to generate a peristaltic-like effect for liquid pumping. The fabrication process was similar to microvalve fabrication as mentioned earlier.

In order to investigate the frequency response time of the micropump, the effect of two actuation frequencies of 3.3 Hz and 5 Hz on pumping flow rate was investigated. An in house-developed air pump with adjustable actuation frequency was used to actuate the diaphragms. Pumping flow rate decreased from 89±6 µl/min to 65±5 µl/min as the actuation frequency dropped from 5 to 3.3 Hz using 20 kPa air pressure for actuation. This decline in the flow rate can be associated with the longer residence time of the flow in the pumping chambers at lower frequency of actuation.

Also, the impact of downstream pressure at the discharge port on the overall pumping rate was investigated. The test setup had one liquid column at the suction port and one liquid column at the discharge port. By changing the difference between the heights of the two liquid columns, the pressure at the discharge port was controlled. In order to measure the flow rate, the liquid pumped to the discharge column was collected by a 1 ml syringe from the highest point of the discharge column in a given time. As the downstream pressure at the discharge port was increased from 12 mm to 42 mm, pumping flow rate was decreased from 82 µl/min to 55 µl/min, Figure 7(d).

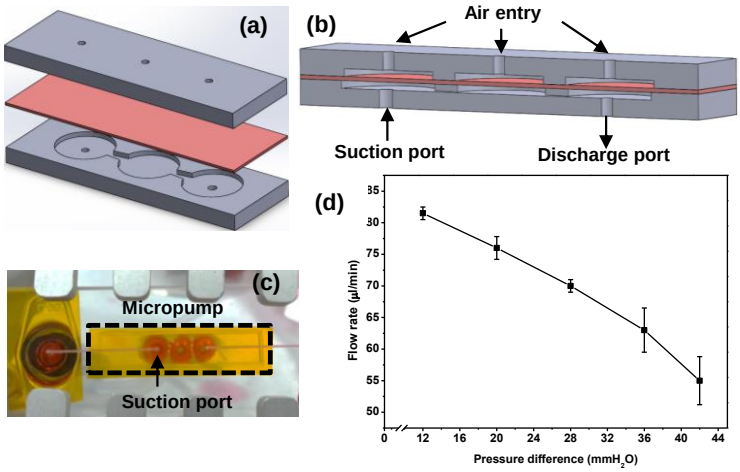

Figure 7. (a) A schematic of cross-sectional view of the micropump comprised of three interconnected liquid chambers integrated on a single substrate. (b) The bottom view of a fabricated micropump integrated on a test chip using Kapton tape. (c) Pumping flow rate vs. pressure difference between suction and discharge ports of the micropump, frequency of diaphragm actuation is 5 Hz with actuation air pressure of 20 kPa.

Conclusions

This paper reported the fabrication and characterization of an air actuated normally-open microvalve and a micropump made of thermoplastics. Microvalves could withstand liquid pressures of up to 600 kPa with no burst failure. Also, leakage-free operation at liquid pressures lower than the air pressure was realized. Characterization results proved that the microvalve can be used for controlling both liquid flows and electrical fields. No particular surface treatment used for bonding process. The plug-and-play microvalves and micropumps can be easily sterilized and autoclaved for cell-based microfluidic devices and microfluidic organ-on-chip platforms. Multiple valves can be integrated into one microfluidic device and provide complex flow manipulation functions. Fabricated microvalves with the embedded chip-to-world connectors are simple to operate. Such design features make them as off-the-shelf functional elements with easy integration onto thermoplastic microfluidic chips. Exploited materials and the proposed fabrication process are appropriate for mass production of microfluidic components and circuitries using thermoforming process, particularly injection molding method. In addition, other thermoplastic materials including COC and PC with respective T_g of 80 ºC and 148 ºC Gärtner 2008) can be explored for bonding to TPU film to make the proposed functional elements.

References

Becker H, Gärtner C (2008) Polymer microfabrication technologies for microfluidic systems. Anal Bioanal Chem 390:89–111. doi: 10.1007/s00216-007-1692-2

Berthier E, Young EWK, Beebe D (2012) Engineers are from PDMS-land, Biologists are from Polystyrenia. Lab Chip 12:1224–1237. doi: 10.1039/c2lc20982a

Byrne MB, Leslie MT, Gaskins HR, Kenis PJA (2014) Methods to study the tumor microenvironment under controlled oxygen conditions. Trends Biotechnol 32:556–63. doi: 10.1016/j.tibtech.2014.09.006

Chin CD, Linder V, Sia SK (2012) Commercialization of microfluidic point-of-care diagnostic devices. Lab Chip 12:2118–2134. doi: 10.1039/c2lc21204h

Elizabeth Hulme S, Shevkoplyas SS, Whitesides GM (2009) Incorporation of prefabricated screw, pneumatic, and solenoid valves into microfluidic devices. Lab Chip 9:79–86. doi: 10.1039/b809673b

Frimat J-P, Becker M, Chiang Y-Y, et al (2011) A microfluidic array with cellular valving for single cell co-culture. Lab Chip 11:231–237. doi: 10.1039/c0lc00172d

Gómez-Sjöberg R, Leyrat AA, Pirone DM, et al (2007) Versatile, fully automated, microfluidic cell culture system. Anal Chem 79:8557–8563. doi: 10.1021/ac071311w

Grover WH, von Muhlen MG, Manalis SR (2008) Teflon films for chemically-inert microfluidic valves and pumps. Lab Chip 8:913–918. doi: 10.1039/b800600h

Gu P, Liu K, Chen H, et al (2010) Chemical-Assisted Bonding of Thermoplastics/Elastomer for Fabricating Microfluidic Valves. Anal Chem 83:446–452. doi: 10.1021/ac101999w

Gu P, Nishida T, Fan ZH (2013) The use of polyurethane as an elastomer in thermoplastic microfluidic devices and the study of its creep properties. Electrophoresis n/a–n/a. doi: 10.1002/elps.201300160

Hong TF, Ju WJ, Wu MC, et al (2010) Rapid prototyping of PMMA microfluidic chips utilizing a CO2 laser. Microfluid Nanofluidics 9:1125–1133. doi: 10.1007/s10404-010-0633-0

Hulme SE, Shevkoplyas SS, McGuigan AP, et al (2010) Lifespan-on-a-chip: microfluidic chambers for performing lifelong observation of C. elegans. Lab Chip 10:589–597. doi: 10.1039/b919265d

Irimia D (2010) Microfluidic technologies for temporal perturbations of chemotaxis. Annu Rev Biomed Eng 12:259–284. doi: 10.1146/annurev-bioeng-070909-105241

Jiang L, Erickson D (2013) Light-governed capillary flow in microfluidic systems. Small 9:107–114. doi: 10.1002/smll.201201778

Kang DH, Kim SM, Lee B, et al (2013) Stimuli-responsive hydrogel patterns for smart microfluidics and microarrays. Analyst 138:6230–42. doi: 10.1039/c3an01119d

Lee JN, Park C, Whitesides GM (2003) Solvent Compatibility of Poly(dimethylsiloxane)-Based Microfluidic Devices. Anal Chem 75:6544–6554. doi: 10.1021/ac0346712

Lii J, Hsu W-J, Parsa H, et al (2008) Real-Time Microfluidic System for Studying Mammalian Cells in 3D Microenvironments. Anal Chem 80:3640–3647. doi: 10.1021/ac8000034

Ma H, Jiang L, Shi W, et al (2009) A programmable microvalve-based microfluidic array for characterization of neurotoxin-induced responses of individual C. elegans. Biomicrofluidics. doi: 10.1063/1.3274313

Melin J, Quake SR (2007) Microfluidic Large-Scale Integration: The Evolution of Design Rules for Biological Automation. Annu Rev Biophys Biomol Struct 36:213–231. doi: doi:10.1146/annurev.biophys.36.040306.132646

Nguyen N-T, Huang X, Chuan TK (2002) MEMS-Micropumps: A Review. J Fluids Eng 124:384. doi: 10.1115/1.1459075

Nguyen N-T, Shaegh SAM, Kashaninejad N, Phan D-T (2013) Design, fabrication and characterization of drug delivery systems based on lab-on-a-chip technology. Adv Drug Deliv Rev 65:1403–19. doi: 10.1016/j.addr.2013.05.008

Ochs CJ, Kasuya J, Pavesi A, Kamm RD (2014) Oxygen levels in thermoplastic microfluidic devices during cell culture. Lab Chip 14:459–462. doi: 10.1039/c3lc51160j

Ogilvie IRG, Sieben VJ, Cortese B, et al (2011) Chemically resistant microfluidic valves from Viton® membranes bonded to COC and PMMA. Lab Chip 11:2455–2459. doi: 10.1039/c1lc20069k

Oh KW, Ahn CH (2006) A review of microvalves. J Micromechanics Microengineering 16:R13–R39. doi: 10.1088/0960-1317/16/5/R01

Piccin E, Coltro WKT, Fracassi da Silva JA, et al (2007) Polyurethane from biosource as a new material for fabrication of microfluidic devices by rapid prototyping. J Chromatogr A 1173:151–158. doi: http://dx.doi.org/10.1016/j.chroma.2007.09.081

Qin L, Vermesh O, Shi Q, Heath JR (2009) Self-powered microfluidic chips for multiplexed protein assays from whole blood. Lab Chip 9:2016–2020. doi: 10.1039/b821247c

Regehr KJ, Domenech M, Koepsel JT, et al (2009) Biological implications of polydimethylsiloxane-based microfluidic cell culture. Lab Chip 9:2132–2139. doi: 10.1039/b903043c

Shiraki Y, Tsuruta K, Morimoto J, et al (2015) Preparation of Molecule-Responsive Microsized Hydrogels via Photopolymerization for Smart Microchannel Microvalves. Macromol Rapid Commun 36:515–519. doi: 10.1002/marc.201400676

Tsao CW, DeVoe DL (2009) Bonding of thermoplastic polymer microfluidics. Microfluid. Nanofluidics 6:1–16.

Unger MA, Chou HP, Thorsen T, et al (2000) Monolithic microfabricated valves and pumps by multilayer soft lithography. Science 288:113–116. doi: 10.1126/science.288.5463.113

Waldbaur A, Rapp H, Länge K, Rapp BE (2011) Let there be chip—towards rapid prototyping of microfluidic devices: one-step manufacturing processes. Anal. Methods 3:2681.

Weibel DB, Kruithof M, Potenta S, et al (2005) Torque-Actuated Valves for Microfluidics. Anal Chem 77:4726–4733. doi: 10.1021/ac048303p

Wu H, Wheeler A, Zare RN (2004) Chemical cytometry on a picoliter-scale integrated microfluidic chip. Proc Natl Acad Sci U S A 101:12809–12813. doi: 10.1073/pnas.0405299101

Wu MH, Huang SB, Cui Z, et al (2008) Development of perfusion-based micro 3-D cell culture platform and its application for high throughput drug testing. Sensors Actuators, B Chem 129:231–240. doi: 10.1016/j.snb.2007.07.145

Wu W-I, Sask KN, Brash JL, Selvaganapathy PR (2012) Polyurethane-based microfluidic devices for blood contacting applications. Lab Chip 12:960–970. doi: 10.1039/c2lc21075d

Yobas L, Tang K-C, Yong S-E, Kye-Zheng Ong E (2008) A disposable planar peristaltic pump for lab-on-a-chip. Lab Chip 8:660–662. doi: 10.1039/b720024b

Zeng S, Li B, Su X, et al (2009) Microvalve-actuated precise control of individual droplets in microfluidic devices. Lab Chip 9:1340–1343. doi: 10.1039/b821803j

Zhang W, Lin S, Wang C, et al (2009) PMMA/PDMS valves and pumps for disposable microfluidics. Lab Chip 9:3088–3094. doi: 10.1039/b907254c

Zhang X, Chen Z, Huang Y (2015) A valve-less microfluidic peristaltic pumping method. Biomicrofluidics 9:014118. doi: 10.1063/1.4907982

Zhu CH, Lu Y, Peng J, et al (2012) Photothermally sensitive poly(N-isopropylacrylamide)/graphene oxide nanocomposite hydrogels as remote light-controlled liquid microvalves. Adv Funct Mater 22:4017–4022. doi: 10.1002/adfm.201201020